COMMUNICATION

Quantum Dots Assembled from an Aziridinium Based Hybrid Perovskite Displaying Tunable Luminescence

Received 00th January 20xx,
Accepted 00th January 20xx

DOI: 10.1039/x0xx00000x

Oleksandr A. Semenikhin,[a] Olesia I. Kucheriv,[a] Liviu Sacarescu,[b] Sergiu Shova[b] and Il'ya A. Gural'skiy*[a]

3D hybrid perovskites based upon small organic cations gave start to a new intensively growing class of semiconducting materials. Here we report on the elaboration of quantum dots of a recently emerged new perovskite (AzrH)$PbBr_3$ (AzrH = aziridinium cation). By employing the antisolvent precipitation technique and stabiliztion with a cationic surfactant we succeded to obtain quantum dots that display tunable luminescence. This piece of work shows the perspective of aziridinium based materials for the elaboration of advanced photonic nanostructures.

3D cubic hybrid organic-inorganic perovskites with ABX_3 composition where A is an organic cation, B is a metal cation and X is a halogen anion attract considerable attention due to their semiconducting properties. For example, these materials have already been used for production of solar cells[1], in lasers[2], LEDs[3], as scintillators[4], for X-ray detection[5] etc.

3D hybrid perovskites demand small organic cations to fulfil geometric requirements and very few of them with appropriate size are known. The most studied and applied 3D hybrid perovskites for today are $MAPbHal_3$ and $FAPbHal_3$, where MA = methylammonium,[6] FA = formamidinium,[7] Hal = Cl, Br and I. As well, methylhydrazinium (MHy) is able to support 3D structure of (MHy)$PbCl_3$[8–11] and (MHy)$PbBr_3$[10–12], and fluoromethylammonium of $FCH_2NH_3PbBr_3$[13].

At first glance the properties of cubic 3D hybrid perovskites are similar independently on the cation, however many important achievements were reached exactly via the organic cation variation, namely higher solar cell harvesting efficiency,[14] suppression of polymorphism,[15] photoluminescence band shifting,[16] appearance of non-linear optical properties[8,12].

Recently we reported on the synthesis of new compounds (AzrH)$PbHal_3$ (AzrH = aziridinium cation, Hal = Cl, Br, I) which appeared to be classic semiconducting cubic perovskites.[17] Raman and photoluminescence studies of (AzrH)$PbHal_3$ bulk perovskites were also reported.[18] Considering a substantial role of a cation towards further applicability we targeted newly emerged aziridinium perovskites and here we report on a preparation of quantum dots (QDs) based on (AzrH)$PbBr_3$ and analyze their photophysical properties. In this work we offer a route towards a new functional form of (AzrH)$PbBr_3$ which may be suitable for further applications.

Figure 1 depicts schematic representation of (AzrH)$PbBr_3$ QDs (**Br-QDs**) preparation with a cetyltrimethylammonium bromide (CTAB) used for stabilization. In a typical procedure, CTAB and (AzrH)$PbBr_3$ were dissolved in toluene and dimethyl sulfoxide (DMSO), respectively (step I). It is worth noting that aziridinium is a very reactive species (compared to MA and FA), thus the solution of perovskite in DMSO was used immediately after preparation. Then CTAB solution was added to the perovskite solution (step II) in order to form separate particles according to the antisolvent-solvent precipitation technique in presence of a lipophilic surfactant. Intensive mixing allows to convert almost all of the perovskite into QDs (step III). As in most other syntheses,[19] the surfactant forms an outer shell, which makes quantum dots more stable. Since CTAB is taken in excess it is required to purify solution from the surfactant, that is done by centrifugation (step IV). Further, toluene is added and colloid is obtained by ultrasonicfication (step V). Worth noting, we have alternatively tried to synthesise aziridinium based QDs in inverse microemulsions, however this procedure was found to be inefficient. While nanoparticles are initially formed in the acidic nanodroplets they appear to be unstable at low pH and are destroyed within ca. 5 min. That is why non-aqueous media were selected for the target synthesis.

The successfully obtained **Br-QDs** in toluene were deposited on a TEM grid and their microscopic image is shown in Figure 2a. The largest formations obtained by this method do not exceed the size of 15 nm. Based on the observed QDs, a histogram of size distribution can be built (Figure 2b) and it corresponds well to the log-normal distribution. The average size of observed **Br-QDs** is 8.6 ± 1.2 nm.

[a] *Department of Chemistry, Taras Shevchenko National University of Kyiv, Volodymyrska St. 64, Kyiv 01601, Ukraine. E-mail: illia.guralskyi@univ.kiev.ua*
[b] *Department of Inorganic Polymers, Petru Poni Institute of Macromolecular Chemistry, Aleea Grigore Ghica Voda 41-A, Iasi 700487, Romania*

† *Electronic supplementary information (ESI) available: Synthetic procedures, physical characterization details, IR spectrum. For ESI see DOI:*

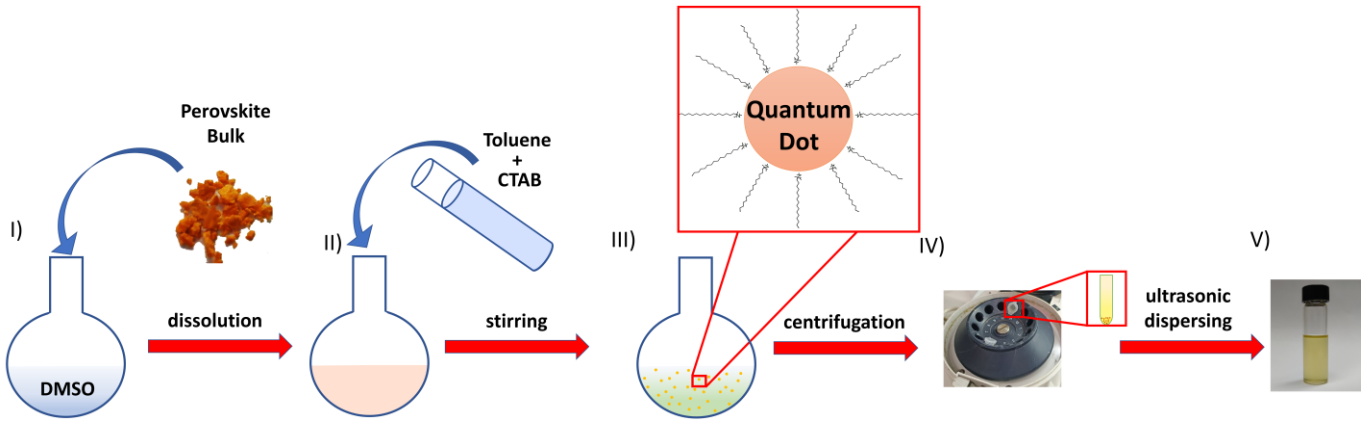

Figure 1. Schematic representation of the **Br-QDs** elaboration. (I) Perovskite is dissolved in DMSO; (ii) CTAB solution in toluene is added to perovskite solution in DMSO; (iii) Nanoparticles are precipitated by an antisolvent in the presence of a surfactant; (iv) QDs are separated from the reaction mixture by centrifugation; (v) QDs are re-dispersed in an organic solvent.

For some comparison, QDs of $CsPbBr_3$ with an average diameter of 11.9 nm are obtained by a precipitation method.[20] At the same time, in the first report of solution-based synthesis of $MAPbBr_3$ the size of nanoparticles is 6 nm.[21]

Solvent free QDs can be obtained from the colloidal solution by centrifugation affording an orange solid shown in Figure 2c, which has a typical appearance of bromide 3D hybrid perovskites. Its powder X-ray diffraction (PXRD) pattern shows the predominant $(AzrH)PbBr_3$ phase (Figure 2d) with some admixture of CTAB. Importantly, despite the high reactivity of $AzrH^+$ species, the proposed experimental technique allows to produce $(AzrH)PbBr_3$ QDs and avoid a hydrobromination of aziridine.

Considering a semiconducting nature of the title perovskite, the colloid of nanoparticles in toluene were studied via UV-Vis and fluorescent spectroscopies. The corresponding absorption spectrum is shown in Figure 3a. While there is a typical wavelength-dependent scattering, one can observe an increase of absorption from 550 nm, that evidences the presence of an optical band gap. This optical behaviour corroborates well with optical properties of the bulk $(AzrH)PbBr_3$ perovskite.[17] Considering $(AzrH)PbBr_3$ is a direct-bandgap semiconductor, to estimate the optical band gap value we have used a Tauc $(\alpha h\nu)^2$ approximation (see Figure 3b). The extracted value is 2.25 eV is almost identical to the one of the bulk; it is comparable with the closest analogous QDs based on 3D lead bromide perovskites, e.g. $MAPbBr_3$ (2.3 eV)[22] and $CsPbBr_3$ (2.30 eV).[23] This indicates that the obtained nanosized material may have an outstanding potential towards photovoltaic and optoelectronic applications and significantly contribute to the extension of available narrow set of 3D hybrid perovskite nanomaterials.

As a typical property of QDs, the title nanomaterials exhibit a photoluminescence upon excitation with higher energy photons. Emission and excitation spectra of the QDs in toluene measured at room temperature are shown in Figure 4a. Upon excitation at 350 nm QDs show a narrow emission peak at 520 nm (FWHM is 32 nm). Both the peak position and FWHM of $(AzrH)PbBr_3$ QDs are similar to those, found for the first $MAPbBr_3$ nanoparticles obtained by solution-based synthesis. For $MAPbBr_3$ the corresponding values varied slightly for nanoparticles obtained by different synthetic approaches and were in the range of 524-530 nm and 21-23 nm for peak position and FWHM, respectively.[21]

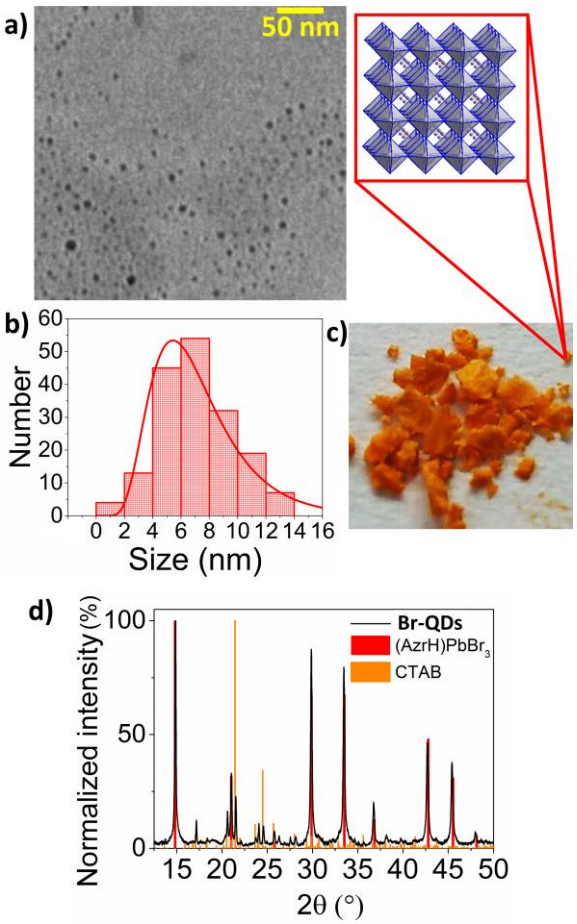

Figure 2. (a) TEM image of **Br-QDs;** (b) Histogram of their size distribution; (c) Macroscopic photographs of precipitated and dried QDs; d) Experimental PXRD pattern of dried QDs (black line) in comparison with theoretical patterns of $(AzrH)PbBr_3$[17] (red bars) and CTAB[24] (orange bars) showing phase composition of the obtained nanomaterial. (Insert) Crystal structure of the $(AzrH)PbBr_3$ perovskite.

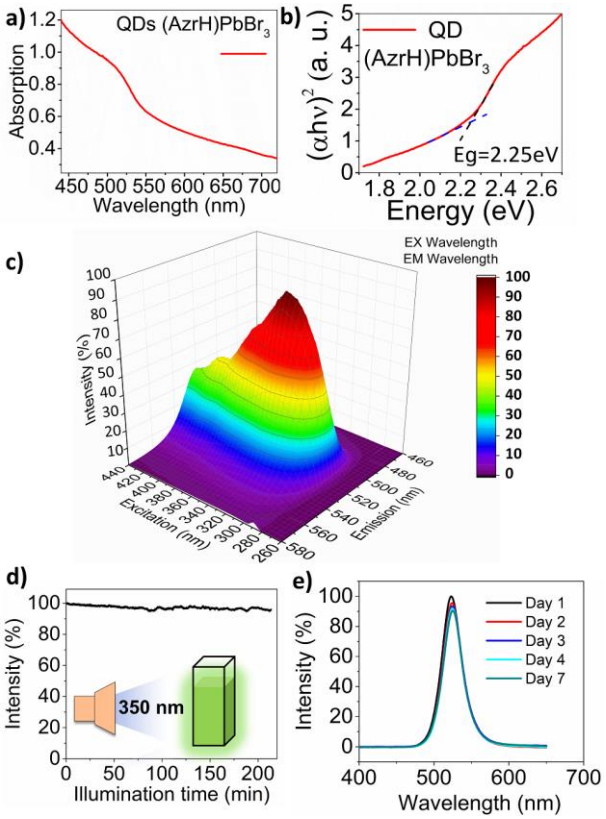

Figure 3. Optical properties of **Br-QDs** colloidal solution in toluene: (a) UV-Vis spectrum in the range 440-720 nm; (b) Tauc plot obtained from the UV-Vis spectrum; (c) 3D photoluminescence spectrum; (d) Photoluminescence of **Br-QDs** as a function of illumination time (λ_{EX} = 350 nm, λ_{EM} = 515 nm). (e) Photoluminescence of **Br-QDs** measured within 7 consequent days showing stability of the obtained material.

Green emission of $(AzrH)PbBr_3$ can be followed visually as shown on the insert in Figure 4a. Photoluminescence excitation is characterized by a wide band ascending from 280 nm with a maximum at c.a. 320 nm. These ranges are also well seen on a 3D photoluminescence spectrum given in Figure 3c. While there is a wide wavelength range available for the excitation there is a single peak emission in the green part of the spectrum. For comparison, photoluminescence spectra of bulk $(AzrH)PbBr_3$ obtained by Mączka et al.[18] display multiple emission peaks with the most intensive one located at 574 nm at 80 K. The peaks undergo temperature dependent blue-shifts upon cooling to room temperature with the most intensive one reaching ca. 530 nm, that is consistent with result obtained in this work. In case of $FAPbBr_3$ and $MAPbBr_3$ QDs, positions of photoluminescence peaks at room temperature usually can be found in the range of ca. 520-530 nm[25,26] and 513-530 nm[21,27], respectively, depending on the size and synthesis method. For the bulk samples these value are ca. 544-547 nm[28] ($FAPbBr_3$) and 530 nm[29] ($MAPbBr_3$). Thus, in MA and FA analogues processing towards QDs usually leads to a slight blue-shift of photoluminescence peak similar to results found in this work.

The photoluminescence quantum yield was estimated to be 13.7% by comparison with a standard sample quinine sulphate (for procedure description see ESI).[30] The obtained quantum yield value may be lower than those achieved with $MAPbBr_3$ and $CsPbBr_3$ nanoparticles for today. However, the quantum yield in the first reported $MAPbBr_3$ was 17%[21] which was soon significantly improved by the same team to 83%[27] by tuning the molar ratio between precursors. Thus, the obtained material widens the possibilities for hybrid perovskite-based optoelectronic and photovoltaic domains beyond already well-studied MA and FA analogues and creates brand new directions for further research in the field.

Photostability of **Br-QDs** was studied using fluorimeter lamps as a light source (λ_{EX} = 350 nm). As shown in Figure 3d within the first hour of constant illumination photoluminescence emission intensity (measured at λ_{EM} = 515 nm) of **Br-QDs** dropped by 2.4%. Within 3.5 hours of experiment the maximum loss of photoluminescence intensity reached 4.2 %, which is a satisfactory value for hybrid perovskite QDs. For comparison, toluene dispersion of 5.5±1.5 nm $MAPbI_3$ nanoparticles obtained by antisolvent precipitation in the presence of octylammonium bromide and 1-octadecene displayed 7% emission intensity loss in the first 30 min of illumination by 350 nm radiation and additional loss of 10% after the following 481 min.[27]

In order to prove that **Br-QDs** are chemically stable, emission spectra of the obtained colloidal solution were measured within 7 consequent days (Figure 3e) and showed that photoluminescence intensity dropped by 9.6% after this period of time. For comparison, $FAPbBr_3$ quantum dots obtained with assistance of oleic acid and octadecene displayed similar stability upon storage within 7 days and were shown to lose 55% of emission intensity within one month.[31] The performed photo- and chemical stability measurements show that despite the instability of aziridinium itself, its incorporation into a perovskite framework results in the formation of a material, which is relatively stable at ambient conditions. As well, encapsulation with CTAB plays an important role in the nanomaterial stabilization as synthesis of $(AzrH)PbBr_3$ in the same conditions without CTAB addition leads to the formation of non-luminescent submicronic crystals 0.2-0.8 µm in size (Figure S2), but not QDs.

The emission wavelength of QDs can also be tuned by mixing different halogens, since their optical bandgap depends on the halogen used (Figure 4). Photoluminescence spectra of $(AzrH)PbCl_xBr_{3-x}$ (**ClBr-QDs**; where x = 1.7 according to precursors ratio) display a blue shift of the emission peak to 462 nm (FWHM = 25 nm). Thus, partial substitution of Br anions with Cl anions allowed to tune emission maximum by 58 nm. Similar to **Br-QDs**, photoluminescence excitation of **ClBr-QDs** is characterized by a wide band ascending from 280 nm with a maximum at c.a. 330 nm. TEM image of **ClBr-QDs** and histogram of their size distribution is shown in Figures 4b,c. The average size of these QDs is 8 ± 2 nm. Importantly, a red-shift of the emission band is also possible via a partial substitution of bromine by iodine (see Figure S3 in the ESI).

In conclusion, we have developed excusive QDs from a recently emerged aziridinium cation-based perovskites. The elaborated synthetic procedure utilizes an ability of CTAB to stabilize small (ca. 9 nm) $(AzrH)PbBr_3$ nanoparticles.

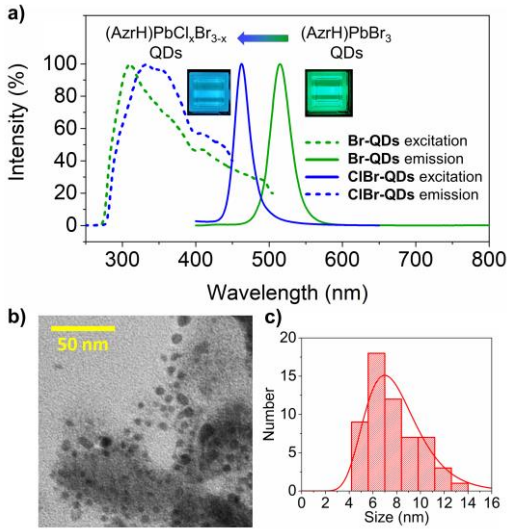

Figure 4. (a) Emission spectra (solid lines; λ_{EX}**Br-QDs** = 350 nm, λ_{EX}**ClBr-QDs** = 350 excitation wavelength 350 nm) and excitation spectra dashed lines; λ_{EM}**Br-QDs** = 520 nm, λ_{EM}**ClBr-QDs** = 462 nm); (Insert) Photos of **ClBr-QDs** (blue) and **Br-QDs** (green) under 350 nm light. (b) TEM image of **ClBr-QDs**. (c) Histogram of **ClBr-QDs** size distribution.

The obtained nanoparticles are characterized by green emission luminescence and display satisfactory chemical and photostability. It was shown that QDs' emission can be blue-shifted via bromide substitution with chloride by 58 nm. Moreover, mixing small cations for the perovskite material design was shown to be effective for the optimisation of functional materials and this approach can be further used with aziridinium-based QDs. Thus, QDs based on this perovskite have a large gate of available variations and many more unique materials can be created.

Authors acknowledge the financial support from the Ministry of Education and Science of Ukraine and the courage of Armed Forces of Ukraine that made the submission of this manuscript possible.

Conflicts of interest

There are no conflicts to declare.

References

1 M. A. Green, A. Ho-Baillie and H. J. Snaith, *Nat. Photonics*, 2014, **8**, 506–514.
2 B. R. Sutherland and E. H. Sargent, *Nat. Photonics*, 2016, **10**, 295–302.
3 Y. Yin, Z. Hu, M. U. Ali, M. Duan, L. Gao, M. Liu, W. Peng, J. Geng, S. Pan, Y. Wu, J. Hou, J. Fan, D. Li, X. Zhang and H. Meng, *Adv. Mater. Technol.*, 2020, **5**, 2000251.
4 Q. Chen, J. Wu, X. Ou, B. Huang, J. Almutlaq, A. A. Zhumekenov, X. Guan, S. Han, L. Liang, Z. Yi, J. Li, X. Xie, Y. Wang, Y. Li, D. Fan, D. B. L. Teh, A. H. All, O. F. Mohammed, O. M. Bakr, T. Wu, M. Bettinelli, H. Yang, W. Huang and X. Liu, *Nature*, 2018, **561**, 88–93.
5 H. Wei, Y. Fang, P. Mulligan, W. Chuirazzi, H. Fang, C. Wang, B. R. Ecker, Y. Gao, M. A. Loi, L. Cao and J. Huang, *Nat. Photonics*, 2016, **10**, 333–339.
6 6 D. Weber, *Zeitschrift für Naturforsch. B*, 1978, **33**, 1443–1445.
7 C. C. Stoumpos, C. D. Malliakas and M. G. Kanatzidis, *Inorg. Chem.*, 2013, **52**, 9019–9038.
8 M. Mączka, A. Gagor, J. K. Zaręba, D. Stefanska, M. Drozd, S. Balciunas, M. Šimėnas, J. Banys and A. Sieradzki, *Chem. Mater.*, 2020, **32**, 4072–4082.
9 M. Mączka, M. Ptak, D. L. M. Vasconcelos, L. Giriunas, P. T. C. Freire, M. Bertmer, J. Banys and M. Simenas, *J. Phys. Chem. C*, 2020, **124**, 26999–27008.
10 M. Mączka, J. A. Zienkiewicz and M. Ptak, *J. Phys. Chem. C*, 2022, **126**, 4048–4056.
11 D. Drozdowski, A. Gągor, D. Stefańska, J. K. Zaręba, K. Fedoruk, M. Mączka and A. Sieradzki, *J. Phys. Chem. C*, 2022, **126**, 1600–1610.
12 M. Mączka, M. Ptak, A. Gągor, D. Stefańska, J. K. Zaręba and A. Sieradzki, *Chem. Mater.*, 2020, **32**, 1667–1673.
13 S. Huang, P. Huang, L. Wang, J. Han, Y. Chen and H. Zhong, *Adv. Mater.*, 2019, **31**, 1903830.
14 T. Jesper Jacobsson, J.-P. Correa-Baena, M. Pazoki, M. Saliba, K. Schenk, M. Grätzel and A. Hagfeldt, *Energy Environ. Sci.*, 2016, **9**, 1706–1724.
15 L.-Q. Xie, L. Chen, Z.-A. Nan, H.-X. Lin, T. Wang, D.-P. Zhan, J.-W. Yan, B.-W. Mao and Z.-Q. Tian, *J. Am. Chem. Soc.*, 2017, **139**, 3320–3323.
16 C. Otero-Martínez, M. Imran, N. J. Schrenker, J. Ye, K. Ji, A. Rao, S. D. Stranks, R. L. Z. Hoye, S. Bals, L. Manna, J. Pérez-Juste and L. Polavarapu, *Angew. Chemie Int. Ed.*, 2022, **61**, e202205617.
17 H. R. Petrosova, O. I. Kucheriv, S. Shova and I. A. Gural'skiy, *Chem. Commun.*, 2022, **58**, 5745–5748.
18 18 D. Stefańska, M. Ptak and M. Mączka, *Molecules*, 2022, **27**, 7949.
19 S. Ananthakumar and S. Moorthy Babu, *Synth. Met.*, 2018, **246**, 64–95.
20 J. Zhou, H. Lin, Y. Yu, S. Zuo, B. Li and J. Liu, *Chem. – A Eur. J.*, 2020, **26**, 10528–10533.
21 L. C. Schmidt, A. Pertegás, S. González-Carrero, O. Malinkiewicz, S. Agouram, G. Mínguez Espallargas, H. J. Bolink, R. E. Galian and J. Pérez-Prieto, *J. Am. Chem. Soc.*, 2014, **136**, 850–853.
22 D. M. Jang, K. Park, D. H. Kim, J. Park, F. Shojaei, H. S. Kang, J.-P. Ahn, J. W. Lee and J. K. Song, *Nano Lett.*, 2015, **15**, 5191–5199.
23 A. Pramanik, K. Gates, Y. Gao, S. Begum and P. Chandra Ray, *J. Phys. Chem. C*, 2019, **123**, 5150–5156.
24 J. K. Cockcroft, A. Shamsabadi, H. Wu and A. R. Rennie, *Phys. Chem. Chem. Phys.*, 2019, **21**, 25945–25951.
25 Y. Li, T. Ding, X. Luo, Y. Tian, X. Lu and K. Wu, *Chem. Mater.*, 2020, **32**, 549–556.
26 O. Pfingsten, J. Klein, L. Protesescu, M. I. Bodnarchuk, M. V. Kovalenko and G. Bacher, *Nano Lett.*, 2018, **18**, 4440–4446.
27 S. Gonzalez-Carrero, R. E. Galian and J. Pérez-Prieto, *J. Mater. Chem. A*, 2015, **3**, 9187–9193.
28 A. M. El-naggar, M. B. Mohamed, Z. K. Heiba, R. E. Alatawi, A. M. Kamal, A. A. Albassam, Y. Altowairqi and A. Q. Alanazi, *Opt. Mater.*, 2021, **119**, 111318.
29 M. Zhang, H. Yu, M. Lyu, Q. Wang, J.-H. Yun and L. Wang, *Chem. Commun.*, 2014, **50**, 11727–11730.
30 J. W. Eastman, *Photochem. Photobiol.*, 1967, **6**, 55–72.
31 Q. Li, H. Li, H. Shen, F. Wang, F. Zhao, F. Li, X. Zhang, D. Li, X. Jin and W. Sun, *ACS Photonics*, 2017, **4**, 2504–2512.